ORIGINAL PAPER

Cu^{2+}-mediated turn-on fluorescence biosensor based on DNA-templated silver nanoclusters for label-free and sensitive detection of adenosine triphosphate

Jingze Li[1,2] · Guibin Peng[1] · Ying Yu[1] ⬇ · Bixia Lin[1] · Li Zhang[1] · Manli Guo[1] · Yujuan Cao[1] · Yumin Wang[1,3]

Abstract

A Cu^{2+}-mediated turn-on fluorescence biosensor based on the DNA-templated green-emitting silver nanoclusters (DNA@g-AgNCs) was developed for label-free and sensitive detection of adenosine 5′-triphosphate (ATP). Cu^{2+} was able to quench the bright green fluorescence of DNA@g-AgNCs because of the coordination and photoinduced electron transfer between DNA@g-AgNCs and Cu^{2+}. Therefore, a unique and effective fluorescence biosensor can be constructed with the formation of DNA@g-AgNCs/Cu^{2+}/ATP ternary-competition system. With the introduction of ATP, the DNA@g-AgNCs/Cu^{2+} fluorescence sensing system will be disrupted and the fluorescence of DNA@g-AgNCs was recovered due to higher affinity of ATP towards Cu^{2+}. On the basis of this feature, the DNA@g-AgNCs/Cu^{2+} fluorescence sensing system demonstrated quantitative determination of ATP in the range 0.05 - 3 μM and a detection limit of 16 nM. Moreover, the fluorescence sensing system was successfully applied to the quantitative determination of ATP in human urine and serum samples with recoveries ranging from 98.6 to 106.5%, showing great promise to provide a label-free, cost-efficient, and rapid platform for ATP-related clinical disease diagnosis.

Keywords Cu^{2+}-mediated fluorescence sensing system · Silver nanoclusters (AgNCs) · Adenosine triphosphate · Label-free detection

Jingze Li and Guibin Peng contributed equally to this work.

✉ Ying Yu
yuyhs@scnu.edu.cn

✉ Yumin Wang
yuminwang@gxnu.edu.cn

1 Guangzhou Key Laboratory of Analytical Chemistry for Biomedicine, School of Chemistry, South China Normal University, Guangzhou, Guangdong 510006, People's Republic of China

2 School of Materials Engineering, Jiangxi College of Applied Technology, Ganzhou, Jiangxi 341000, People's Republic of China

3 State Key Laboratory for the Chemistry and Molecular Engineering of Medicinal Resources, School of Chemistry and Pharmaceutical Sciences, Guangxi Normal University, Guilin, Guangxi 541004, People's Republic of China

Introduction

Multifunctional nucleoside polyphosphates including adenosine 5′-triphosphate (ATP) play a pivotal role in metabolic processes of living organisms [1–4]. The abnormal concentration of ATP in biological system has found to be closely associated with many clinical disorders and diseases [5–8]. In this regard, developing a rapid, simple, and effective sensing method for the quantitative determination of the ATP is undoubtedly of great importance in biochemical study and clinical diagnosis. Until now, various kinds of analytical techniques, which include electrochemical method [9–11], high-performance liquid chromatography [12–14], nuclear magnetic resonance spectroscopy [15, 16], and capillary electrophoresis [17, 18], have been developed for the detection of ATP and these analytical methods showed high sensitivity and selectivity towards ATP. In recent years, various fluorescence methods with the assistance of kinds of nanomaterials, such as quantum dots, copper nanoparticles, metal–organic frameworks, and magnetic nanoparticles, have also been proposed in the quantitative determination

Scheme 1 Schematic illustration of the construction of DNA@g-AgNCs/Cu²⁺ fluorescence sensing system and its application for ATP detection
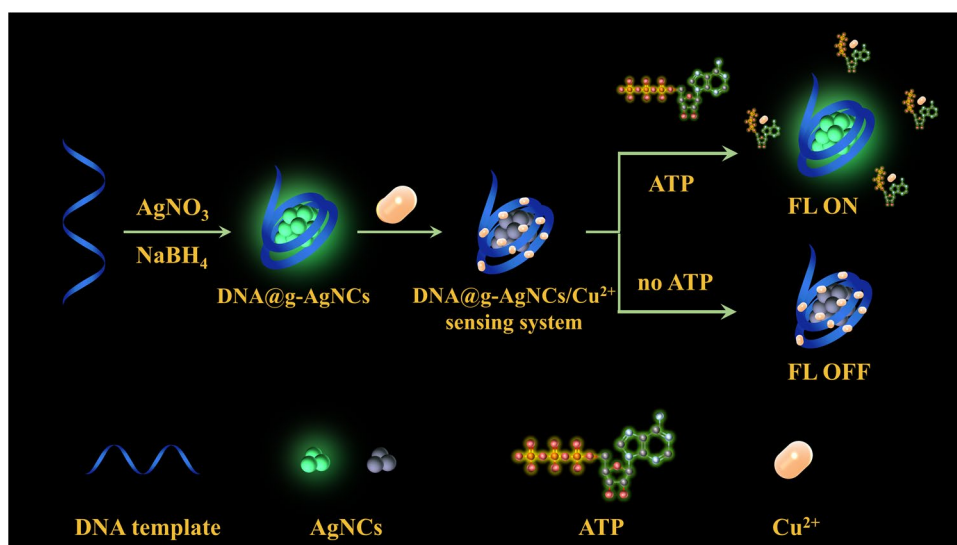
of ATP due to its high sensitivity, convenience, simplicity, real-time, and fast response [19–23]. Nevertheless, these fluorescent strategies were not able to circumvent some shortcomings including time-consuming and complicated probe preparation.

In the past decade, luminescent noble-metal (Au, Ag, Cu, and so forth) nanoclusters, consisting of several to hundreds of metal atoms with a particle size ranging from 2 to 10 nm, have found wide application in a variety of research fields [24–26]. Particularly, silver nanoclusters (AgNCs) have aroused more and more attention due to their advantages of relatively low cost, simple synthesis procedure, good biocompatibility, and adjustable emission wavelength [27–29]. To date, several fluorescence assays have also been reported for the detection of ATP with assistance of DNA-templated silver nanocluster (DNA@AgNCs) [30–33]. As reported in these research work, the sensing mechanisms for ATP detection were based on ATP-caused DNA conformation switching or ATP-induced fluorescence alteration of DNA@AgNCs. However, the interaction between DNA-templated silver nanocluster (DNA@AgNCs) and metal ion has not been investigated. In addition, the construction of fluorescence biosensor based on DNA@AgNCs and metal ion for ATP sensing was not previously reported.

Herein, a novel fluorescence sensing system based on DNA-templated silver nanocluster (DNA@g-AgNCs) for sensitive and label-free detection of ATP in biological fluids was developed. As illustrated in Scheme 1, first, green-emitting AgNCs (g-AgNCs) are formed on DNA template in the presence of $AgNO_3$ and reductant $NaBH_4$. Then, the DNA@g-AgNCs/Cu²⁺ fluorescence sensing system is constructed by the incubation of DNA@g-AgNCs with Cu²⁺ through the chelation of DNA towards Cu²⁺. With the formation of the sensing system, the bright green fluorescence emitted by g-AgNCs were effectively quenched by Cu²⁺ via photoinduced electron transfer (PET). When the analytical target ATP was introduced, the coordination between Cu²⁺ and DNA@g-AgNCs was prevented due to the higher affinity interaction between ATP and Cu²⁺, leading to a significant recovery of the quenched fluorescence of DNA@g-AgNCs. Therefore, the label-free detection of ATP could be realized by monitoring the fluorescence intensity of DNA@g-AgNCs. Because of the fast and effective fluorescence recovery, this developed fluorescence sensing system will afford a useful nanoplatform for rapid, sensitive, and selective detection of ATP and for related disease diagnosis.

Experimental section

Chemicals and materials

Silver nitrate ($AgNO_3$), sodium borohydride ($NaBH_4$), copper sulfate pentahydrate ($CuSO_4 \cdot 5H_2O$), acetic acid (HAc), sodium acetate (NaAc), orthoboric acid (H_3BO_3), and borax ($Na_2B_4O_7 \cdot 10H_2O$) were purchased from Tianjin Zhiyuan Chemical Reagent Co. Ltd. (Tianjin, China). The DNA oligonucleotide, which was used as the template for the preparation of AgNCs in this work, was PAGE-purified and purchased from Sangon Biotechnology Co. Ltd. (Shanghai, China). The sequences of DNA template are listed as follows: 5′-TGC CTT TTG GGG ACG GAT A-3′. All solutions were prepared with ultrapure water which was purified by Millipore Milli-Q Integral ultrapure water purification system (Billerica, MA, USA) with an electrical resistance of 18.2 MΩ·cm.

Apparatus

The fluorescence spectra were collected by F-4600 fluorescence spectrometer (Hitachi, Japan). The measurement of

UV–vis absorption spectra was performed on a UV-2700 spectrometer (Shimadzu, Japan). The transmission electron microscope (TEM) images and energy-dispersive spectroscopy (EDS) were acquired on JEM-2100HR TEM at an acceleration voltage of 200 kV (JEOL, Japan). Dynamic light scattering (DLS) was measured on a Malvern Nano-ZS particle size analyzer (Malver Instruments, UK). The X-ray photoelectron spectroscopy (XPS) analysis was carried out on an X-ray photoelectron spectrometer (Thermo Fisher, USA). The pH value of all solutions was measured with an FE-28 pH acidity meter (METTLER TOLEDO, Shanghai, China).

Synthesis of green-emitting DNA@g-AgNCs and construction of DNA@g-AgNCs/Cu^{2+} sensing system

The green-emitting DNA@g-AgNCs were synthesized following previously reported procedures with slight modification [34] and the detailed experimental steps for preparing DNA@g-AgNCs is supplied in the Electronic Supporting Material (ESM).

DNA@g-AgNCs/Cu^{2+} sensing system was constructed by the following steps: 30 µL 200 mM HEPES buffer solution (pH 7.4), 50 µL 300 nM copper ion (Cu^{2+}) solution, and 10 µL 3 µM DNA-templated g-AgNC solution were mixed together by using a vortex mixer. Thereafter, the mixture was incubated in water bath at 37 °C for 10 min to fabricate DNA@g-AgNCs/Cu^{2+} sensing system.

Determination of adenosine triphosphate

First, 60 µL of ultrapure water and 150 µL of adenosine triphosphate (ATP) solution with different concentrations were injected into 90 µL of DNA@g-AgNCs/Cu^{2+} sensing system. The mixture was mixed by vortex mixer and incubated in water bath at 37 °C for 30 min. The fluorescence spectra of all the samples were measured in the range from 535 to 700 nm at the excitation wavelength of 505 nm with both excitation and emission slits of 10 nm under a PMT voltage of 700 V.

Detection of ATP in actual samples

Human urine and human serum were selected as actual samples to evaluate the practical applicability of the developed sensing system. Firstly, 5 mL urine sample was centrifuged at 8000 rpm for 10 min. Then, the supernatant was collected and filtered with a 0.22-µm filter membrane. Subsequently, it was diluted 10 times with ultrapure water and stored at 4 °C for further use. Human serum sample was obtained after removing plasma protein in human blood by precipitation. In brief, 1 mL blood sample was vortexed and mixed with 1.5 mL acetonitrile solution at room temperature. After 30 min, the mixture was centrifuged at 10,000 rpm for 10 min. The supernatant was collected and filtered with a 0.22-µm filter membrane. The obtained human serum sample was diluted 10 times with ultrapure water and stored at 4 °C for further use.

The ATP amount in actual samples was subsequently determined with fluorometry and chromatography, respectively. In brief, 100 µL of ATP standard solutions with different concentrations was firstly added to 50 µL of the urine sample or serum sample and the solution was mixed thoroughly by vortexer. For fluorescence analysis method, the total ATP concentrations were measured by using the calibration curve obtained above with standard addition method and fluorescence recovery experiments were performed. For chromatography analysis method, the concentration of ATP was analyzed by high-performance liquid chromatography (HPLC). HPLC was implemented using following experimental conditions: An Inertsil Kromasil-C18 column was equipped with a pump system. The phosphate-buffered solution (pH 7.0) was chosen as the mobile phase. The UV detection wavelength for ATP, the column temperature, and flow rate were set as 259 nm, 30 °C, and 1 mL/min, respectively. ATP in the actual samples was identified by comparison with the retention time of standard samples and the concentrations of ATP were calculated by using the standard method.

Results and discussion

Optimization of the experimental conditions of DNA@g-AgNCs

To obtain DNA@g-AgNCs with intense fluorescence intensity and robust stability, the experimental conditions were firstly optimized. DNA with specific AgNC nucleation sequences was selected as the template. As shown in Fig. 1A, no fluorescence signal was detected in the absence of AgNO$_3$ and reductant NaBH$_4$. In contrast, bright green fluorescence can be obviously seen under the excitation at the wavelength of 505 nm with the addition of AgNO$_3$ and NaBH$_4$, implying that silver ions (Ag$^+$) can bond with the specific base sequence of DNA, and g-AgNCs were formed on the scaffold DNA. In addition, characteristic absorption peak value of DNA@g-AgNCs centered at 500 nm was observed on the UV–vis absorption spectrum [35] (Fig. 1B), further disclosing the successful generation of g-AgNCs on the template DNA.

As reported previously, non-fluorescent Ag nanoparticles would possibly be generated on DNA template under specific conditions [36]. Subsequently, the optimal experimental conditions including the concentration ratio

Fig. 1 A Fluorescence excitation (dashed line) and emission (solid line) spectra of DNA@g-AgNCs (green line) and DNA template (black line). **B** UV–vis absorption spectra of the DNA template (black line) and DNA-templated g-AgNCs (green line). **C** Transmission electron microscopy (TEM). Inset: high-resolution transmission electron microscopy (HRTEM), **D** particle size distribution, **E** dynamic light scattering (DLS), and **F** X-ray electron spectroscopy (XPS) of DNA@g-AgNCs
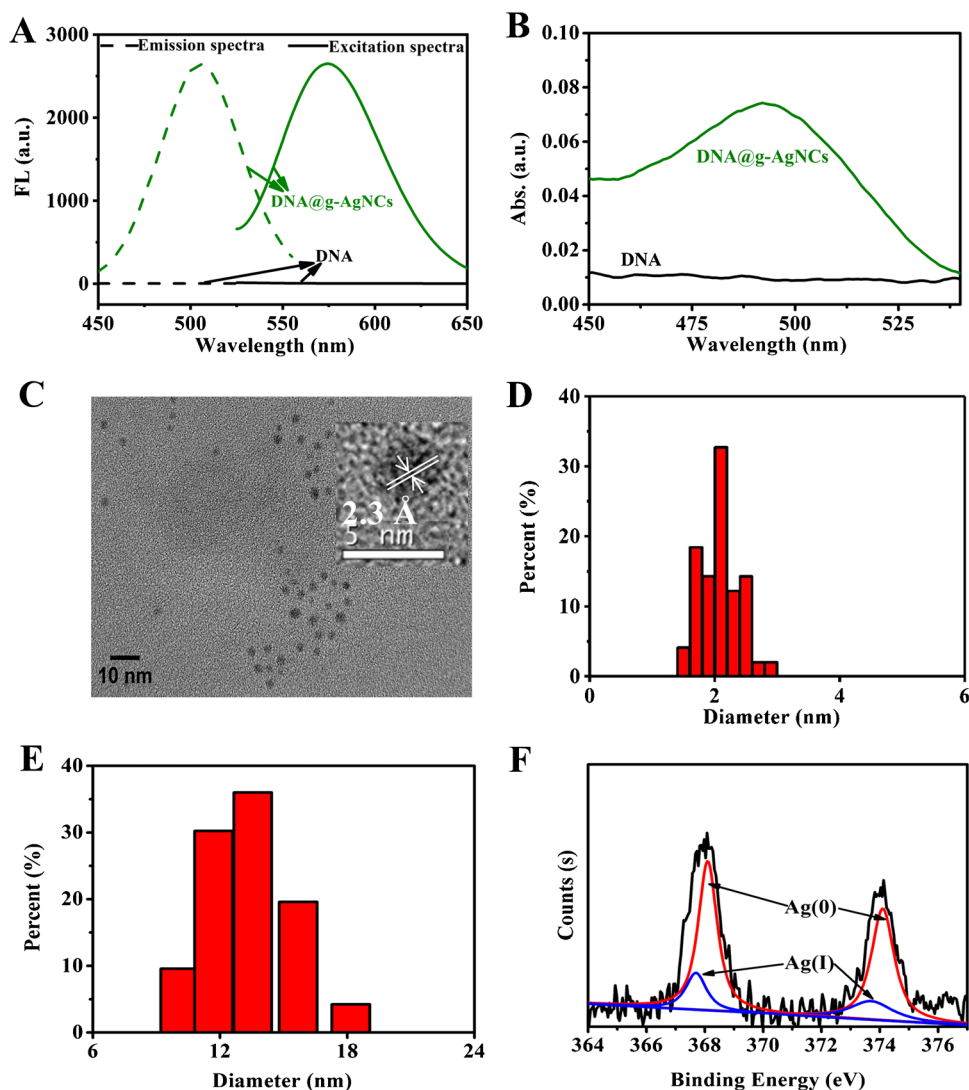
of DNA to silver nitrate, the concentration ratio of silver nitrate to sodium borohydride, reaction time, pH value, reaction buffer, and reaction temperature were investigated. As shown in Figure S1A and S1B, the fluorescence intensity of DNA@g-AgNCs reached the maximum when the concentration ratio of DNA to silver nitrate and silver nitrate to sodium borohydride was 1 to 8 and 1 to 1, respectively. Saturated fluorescence intensity of DNA@g-AgNCs was attained in Figure S1C with reaction time of 4 h, suggesting the redox reaction was sufficiently completed. And it was found that the highest fluorescence intensity of g-AgNCs was obtained with pH value of 7.5, NaAc-HAc buffer solution, and reaction temperature at 4 ℃ (Figure S1D to S1F). Therefore, 1 to 8 concentration ratio (DNA to silver nitrate), 1 to 1 concentration ratio (silver nitrate to sodium borohydride), 4 h reaction time, pH 7.5, NaAc-HAc buffer solution, and 4 ℃ reaction temperature were chosen as the optimal experimental conditions to perform following experiments.

Characterization of DNA@g-AgNCs

Subsequently, the morphology, size, and element content of DNA@g-AgNCs were characterized by using TEM and DLS. TEM image and particle size distribution in Fig. 1C and D show that DNA@g-AgNCs exhibited excellent dispersity and presented a spherical structure scattered with an average size of 1–4 nm. The HRTEM image (inset of Fig. 1C) disclosed that the DNA@g-AgNCs have clear lattice fringes (~ 2.3 Å), which was close to the interplanar distance of the (111) crystal plane of face-centered cubic Ag [37]. DLS revealed that the hydrated average size of the synthesized DNA@g-AgNCs is about 14 nm (Fig. 1E). The in-depth chemical state DNA@g-AgNCs was identified by XPS (Fig. 1F) and two peaks center at 367.8 eV (Ag $3d_{5/2}$) and 374.0 eV (Ag $3d_{3/2}$) were both obviously seen in raw XPS spectra of DNA@g-AgNCs [37]. Furthermore, the deconvolved Ag $3d_{5/2}$ (367.8 eV) and Ag $3d_{3/2}$ (374.0 eV) peaks of XPS spectrum gave four binding energies of 368.1 eV (Ag(0)), 367.7 eV (Ag(I)), 374.1 eV

(Ag(0)), and 373.7 eV(Ag(I)), respectively. The intensities of these four peaks implied that the DNA@g-AgNCs contained about 73.1% Ag(0) and 26.9% Ag(I), indicating that the most of Ag in DNA@g-AgNCs was zero valent. In addition, the signal from Ag was found in elemental analysis of DNA@g-AgNCs by EDS (Figure S2A) and the TEM mapping of the metal distribution proved that the synthetic DNA@g-AgNCs only contained the metallic elements of Ag (Figure S2B to S2D). Taken together, these results demonstrated that DNA@g-AgNCs has been successfully prepared. Furthermore, photostability test was implemented and only slight fluorescence intensity changes were observed after continuous irradiation of g-AgNCs for 2 h and even after 7 days (Figure S3), disclosing that the prepared g-AgNCs have robust photostability.

Verification of the principle of DNA@g-AgNCs/Cu^{2+} sensing system and investigation of fluorescent sensing mechanism

Next, the feasibility of the DNA@g-AgNCs/Cu^{2+} sensing system for detecting ATP was verified using fluorescence analysis. As shown in Fig. 2, Cu^{2+}, ATP and the mixture of Cu^{2+} and ATP were found to exhibit no fluorescence signal under excitation at 505 nm (line 1, line 2, and line 5). In contrast, the prepared DNA@g-AgNCs emits a strong fluorescence peak signal at 575 nm (line 3) and the strong fluorescence signal of DNA@g-AgNCs was dramatically quenched when Cu^{2+} was added (line 4), indicating the successful fabrication of DNA@g-AgNCs/Cu^{2+} sensing system. In addition, the fluorescence intensity of DNA@g-AgNCs remains almost the same after incubation ATP with DNA@g-AgNCs (line 6),
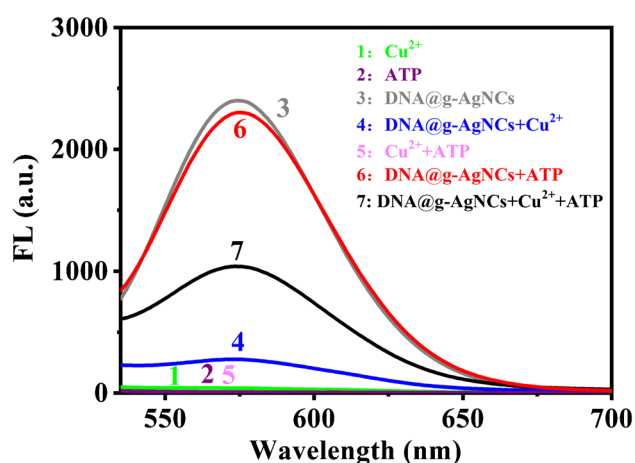
Fig. 2 The fluorescence spectra of Cu^{2+} (line 1, green line), ATP (line 2, purple line), DNA@g-AgNCs (line 3, gray line); DNA@g-AgNCs/Cu^{2+} sensing system (line 4, blue line), Cu^{2+} + ATP (line 5, pink line), DNA@g-AgNCs + ATP (line 6, red line), and DNA@g-AgNCs/Cu.$^{2+}$ sensing system + ATP (line 7, black line)

implying that ATP has no evident effect on the fluorescence properties of DNA@g-AgNCs. With the addition of ATP, the fluorescence signal of DNA@g-AgNCs was recovered and an intense fluorescence peak centered at 575 nm appeared. These experimental results strongly confirmed that a turn-on fluorescence sensing system based on DNA@g-AgNCs/Cu^{2+} was fabricated and it can be applied for label-free detection of ATP.

Subsequently, to understand the interaction and fluorescence quenching mechanism between Cu^{2+} and DNA@g-AgNCs, further investigations were performed by using TEM, DLS, and XPS. After the incubation with Cu^{2+} and DNA@g-AgNCs, copper signal was clearly observed on TEM mapping of the metal distribution (Figure S4), testifying the strong binding between DNA@g-AgNCs and Cu^{2+}. TEM results and particle size distribution in Fig. 3A and B revealed that no smaller- or larger-sized AgNCs (∼2 nm) were generated and the hydrated average size of AgNCs (∼18 nm) remained unchanged (Figure S5A). Moreover, HRTEM image (inset of Fig. 3A) showed that the lattice fringes of these AgNCs (∼2.3 Å) were also in good concordance with that of DNA@g-AgNCs. Additionally, deconvolution of XPS spectra for DNA@g-AgNCs/Cu^{2+} gave two distinct components corresponding to Ag(0) (∼72.20%) and Ag(I) (∼27.8%) (Fig. 3C), which was almost the same with that of DNA@g-AgNCs. All these experimental results evidenced that the physicochemical properties of DNA@g-AgNCs remain invariant after the addition of Cu^{2+}. As reported previously, DNA has a high affinity towards Cu^{2+} [38]. Taken together, it was speculated that the fluorescence quenching process may arise from photoinduced electron transfer (PET) [39–41].

Further, the morphology, size, and element content of AgNCs in DNA@g-AgNCs/Cu^{2+} fluorescence sensing system after the addition of ATP was also examined by TEM, DLS, and XPS. As can be seen in Fig. 3D, E, and F and Figure S5B, the same experimental results were observed as those obtained in the absence or presence of ATP. These results clearly demonstrate that ATP has higher affinity towards Cu^{2+} and the working principle of DNA@g-AgNCs/Cu^{2+} sensing system for ATP detection was also ascribed to the combination between ATP and Cu^{2+}.

In order to obtain the DNA@g-AgNCs/Cu^{2+} fluorescence sensing system with best performance, the buffer solution, incubation temperature, incubation time, and pH value were firstly optimized. According to the experimental results in Figure S6 and Figure S7, HEPES buffer, incubation temperature of 37 °C, incubation time of 10 min, pH 7.4, and 300 nM Cu^{2+} were employed for the preparation of DNA@g-AgNCs/Cu^{2+} in the following experiments.

Sensing performance of DNA@g-AgNCs/Cu^{2+}

To achieve the best sensing performance, the optimized experiment conditions such as reaction temperature, reaction
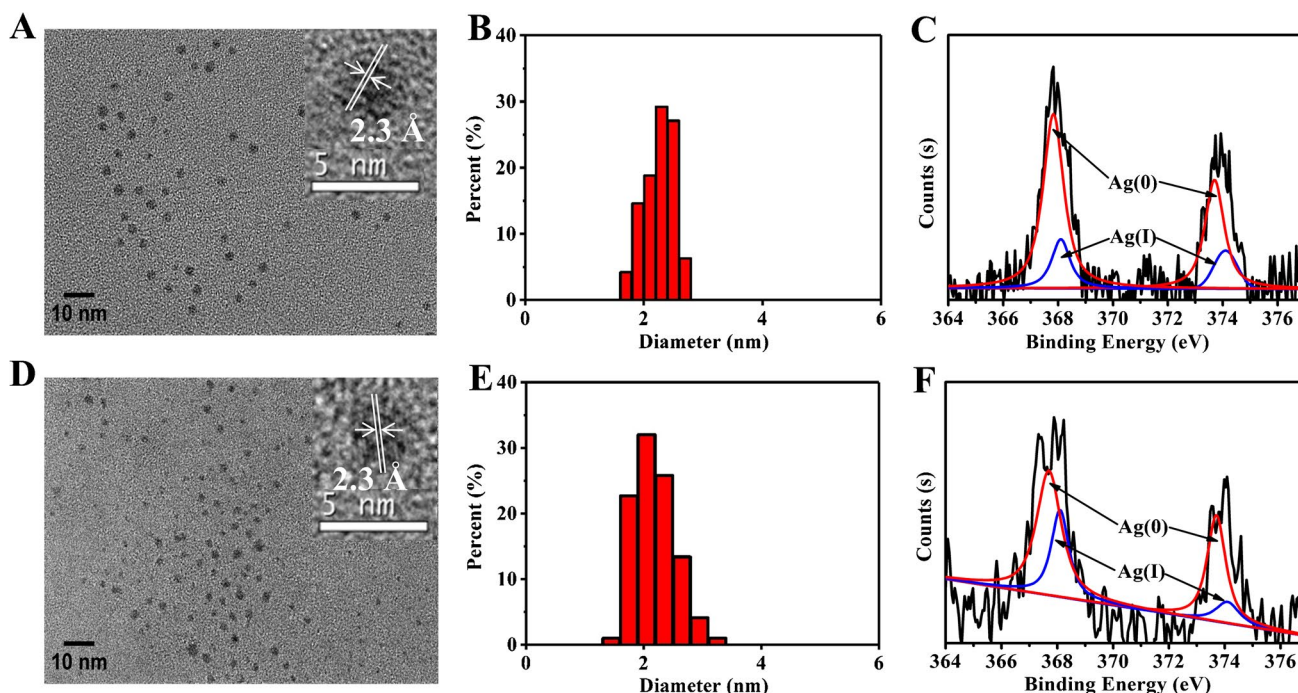
Fig. 3 A Transmission electron microscopy. Inset: high-resolution transmission electron microscopy (HRTEM), **B** particle size distribution, and **C** X-ray electron spectroscopy of DNA@g-AgNCs/Cu^{2+} sensing system. **D** Transmission electron microscopy. Inset: high-res-olution transmission electron microscopy (HRTEM), **E** particle size distribution, and **F** X-ray electron spectroscopy of DNA@g-AgNCs/Cu^{2+} sensing system after incubation with ATP

time, reaction buffer solution, and pH value were then determined. Experimental results in Figure S8 demonstrate incubation temperature of 37 °C, incubation time of 25 min, HEPES buffer, and pH 7.4 which were the optimized experimental conditions.

Next, the quantitative determination of ATP by utilizing DNA@g-AgNCs/Cu^{2+} fluorescence sensing system was implemented under optimized experimental conditions. As shown in Fig. 4A, the fluorescence signal emitted by DNA@g-AgNCs gradually increased with the increasing concentration of ATP. The fluorescence peak values at 575 nm against different concentrations of ATP in the range from 0.05 to 3 μM were then plotted and it was found that the intensity of the fluorescence peak values (F) at 575 nm have a good linear relation to the concentrations of ATP (C_{ATP}) (Fig. 4B). The calibration equation is $F = 422.1 + 186.8 \times C_{ATP}$ and the squared correlation coefficient R^2 is 0.993. According to the 3σ rule, the limit of
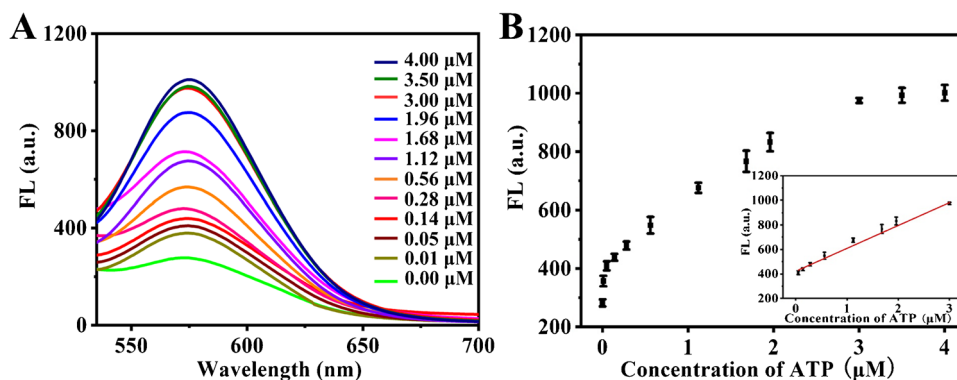

Fig. 4 A Fluorescence spectra of DNA@g-AgNCs/Cu^{2+} sensing system after incubation with varying concentration of ATP (0.00, 0.01, 0.05, 0.14, 0.28, 0.56, 1.12, 1.68, 1.96, 3.00, 3.50, 4.00 μM) in HEPES buffer for 25 min. **B** The relationship corresponding to the fluorescence at 575 nm versus the concentration of ATP ranging from 0 to 4 μM. Inset: linear plot of the fluorescence peak intensity at 575 nm against the concentration of ATP in the range from 0.05 to 3 μM

detection (LOD) of ATP was calculated as 16 nM, which was comparable to or better than some reported fluorescence assays for ATP determination (Table S1). Although some fluorescence methods have higher detection limit, the fluorescent g-AgNCs adopted in this strategy have several advantages including excellent photostability, and low biotoxicity over other fluorophore. Moreover, the construction of this sensing system was one step and this method is label-free and cost-efficient (Table S1).

Determination of ATP in actual samples

In order to further explore the selectivity of the DNA@g-AgNCs/Cu^{2+} towards ATP, various typical anions, glucose, HSA, thrombin, urea, and uric acid were tested. As displayed in Fig. 5, compared with target ATP, these analytes showed no obvious effect on the fluorescence recovery of
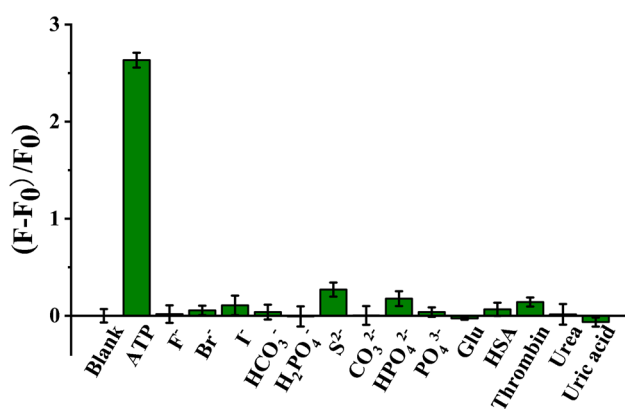
Fig. 5 Selectivity of the DNA@g-AgNCs/Cu^{2+} sensing system for ATP detection. All the concentration of analytical targets (ATP, F^-, Br^-, I^-, HCO_3^-, $H_2PO_4^-$, S^{2-}, CO_3^{2-}, HPO_4^{2-}, PO_4^{3-}, glucose, HAS, thrombin, urea, and uric acid) are 3 μM. F and F_0 are the fluorescence intensities at 575 nm of DNA@g-AgNCs in the presence and absence of analytical target, respectively. Error bars indicate the standard deviations of three repetitive experiments

DNA@g-AgNCs. This finding testified that the DNA@g-AgNCs/Cu^{2+} fluorescence sensing system is selective towards the analytical target ATP and indicated it is feasible for ATP detection of complex real samples. Furthermore, the selectivity against some chemically related species of ATP including ADP, AMP, CTP, GTP, and UTP was also investigated. It can be seen in Figure S9 that chemically related species of ATP except AMP could also recover the fluorescence of the DNA@g-AgNCs/Cu^{2+} sensing system, but ATP has the strongest recovering ability to the fluorescence of DNA@g-AgNCs/Cu^{2+} sensing system.

To assess the practical applicability of the DNA@g-AgNCs/Cu^{2+} fluorescence sensing system, the determination of ATP and a recovery study in human urine and serum samples were performed with a standard addition method. As shown in Table 1, 0.5, 1.0, and 2.0 μM ATP were respectively added in human urine and serum samples, and their recoveries were in the range from 98.6 to 106.5%. In addition, it was clearly observed that the determination values of ATP in human serum and serum samples obtained by the DNA@g-AgNCs/Cu^{2+} sensing system are in good agreement with those of HPLC method, which demonstrate the reliability and accuracy of the established method for ATP quantification in complex actual samples. Nevertheless, this sensing system was not selective towards ATP in the presence of chemically related species of ATP. But for the system containing both ATP and chemically related species of ATP, simultaneous detection of ATP and chemically related species of ATP can be performed according to the previously reported method [42].

Conclusion

A turn-on fluorescence biosensor based on DNA-templated green-emitting AgNCs was proposed for sensitive and label-free detection of ATP with a LOD of 16 nM. Moreover, this fluorescence sensing system worked

Table 1 Determination of ATP in human urine and serum samples

Samples		Spiked ATP (μM)	This strategy			HPLC		
			Found ATP (μM)	Recovery (%)	RSD ($n=3$, %)	Found ATP (μM)	Recovery (%)	RSD ($n=3$, %)
Human urine	1	0.00	ND	—	—	ND	—	—
	2	0.500	0.493	98.6	0.46	0.496	99.2	0.35
	3	1.00	0.988	98.8	1.5	0.994	99.4	1.1
	4	2.00	2.13	107	1.6	2.07	104	0.98
Human serum	1	0.00	ND	—	—	ND	—	—
	2	0.500	0.507	101	0.52	0.504	101	0.68
	3	1.00	0.991	99.1	1.8	1.02	102	1.3
	4	2.00	2.06	103	1.3	2.05	103	0.85

efficiently and stably for determination of the levels of ATP in human serum and urine samples, implying that the proposed biosensor may provide a useful, cost-efficient, and robust approach for ATP-related disease diagnosis and bioanalytical applications. However, this proposed method was not highly selective towards ATP when chemically related species of ATP exists. Our further research work will focus on differentiating ATP and chemically related species of ATP by integrating this sensing strategy and other techniques.

Supplementary Information The online version contains supplementary material available at https://doi.org/10.1007/s00604-022-05617-7.

Data Availability The data sets supporting the results of this article are included within the article and its additional files.

Declarations

Conflict of interest There is no conflict to declare.

References

1. Oakhill JS, Steel R, Chen ZP, Scott JW, Ling NM, Tam S, Kemp BE (2011) AMPK is a direct adenylate charge-regulated protein kinase. Science 332:1433–1435
2. Dong JT, Zhao MP (2016) In-vivo fluorescence imaging of adenosine 5'-triphosphate. Trends Anal Chem 80:190–203
3. Estevez-Herrera J, Dominguez N, Pardo MR, Gonzalez-Santana A, Westhead EW, Borges R, Machado JD (2016) ATP: the crucial component of secretory vesicles. Proc Natl Acad Sci USA 113:E4098–E4106
4. Sigel H, Griesser R (2005) Nucleoside 5'-triphosphates: self-association, acid-base, and metal ion- binding properties in solution. Chem Soc Rev 34:875–900
5. Cai R, Zhang Y, Simmering JE et al (2019) Enhancing glycolysis attenuates Parkinson's disease progression in models and clinical databases. J Clin Invest 129:4539–4549
6. Birk AV, Liu SY, Soong Y, Mills W, Singh P, Warren JD, Seshan SV, Pardee JD, Szeto HH (2013) The mitochondrial-targeted compound SS-31 re-energizes ischemic mitochondria by interacting with cardiolipin. J Am Soc Nephrol 24:1250–1261
7. De Leon DD, Stanley CA (2007) Mechanisms of disease: advances in diagnosis and treatment of hyperinsulinism in neonates. Nat Clin Pract Endocrinol Metab 3:57–68
8. Qu F, Li JW, Han WL, Xia L, You JM (2018) Simultaneous detection of adenosine triphosphate and glucose based on the Cu-Fenton reaction. Sensors 18:2151
9. Lin YZ, Chang TL, Chang CC (2014) Electrochemical method for detecting ATP by 26S proteasome modified gold electrode. Sens Actuators B Chem 190:486–493
10. Li H, Kou BB, Yuan YL, Chai YQ, Yuan R (2022) Porous Fe_3O_4@COF-immobilized gold nanoparticles with excellent catalytic performance for sensitive electrochemical detection of ATP. Biosens Bioelectron 197:113758
11. Zeng JY, Li XX, Wang K, Song JJ, Qi HL (2020) Electrochemical nanoaptasensor for nontinuous monitoring of ATP fluctuation at subcellular level. Anal Chem 92:10940–10945
12. Du LL, Zhang Y, Du Y, Yang DZ, Gao FL, Tang DQ (2015) A novel label-free aptasensor based on target-induced structure switching of aptamer-functionalized mesoporous silica nanoparticles. RSC Adv 5:100960–100967
13. Coolen EJCM, Arts ICW, Swennen ELR, Bast A, Stuart MAC, Dagnelie PC (2008) Simultaneous determination of adenosine triphosphate and its metabolites in human whole blood by RP-HPLC and UV-detection. J Chromatogr B 864:43–51
14. Bao Y, Everaert J, Pietraszkiewicz M, Pietraszkiewicz O, Bohets H, Geise HJ, Peng BX, Nagels LJ (2005) Behaviour of nucleotides and oligonucleotides in potentiometric HPLC detection. Anal Chim Acta 550:130–136
15. Lian YK, Jiang H, Feng JZ, Wang XY, Hou XD, Deng PC (2016) Direct and simultaneous quantification of ATP, ADP and AMP by ^{1}H and ^{31}P nuclear magnetic resonance spectroscopy. Talanta 150:485–492
16. Guo QY, Ren SY, Wang JY, Li Y, Yao ZY, Huang H, Gao ZX, Yang SP (2020) Low field nuclear magnetic sensing technology based on hydrogel-coated superparamagnetic particles. Anal Chim Acta 1094:151–159
17. Liu BF, Ozaki M, Hisamoto H, Luo QM, Utsumi YC, Hattori T, Terabe S (2005) Microfluidic chip toward cellular ATP and ATP-conjugated metabolic analysis with bioluminescence detection. Anal Chem 77:573–578
18. Liu JX, Aerts JT, Rubakhin SS, Zhang XX, Sweedler JV (2014) Analysis of endogenous nucleotides by single cell capillary electrophoresis-mass spectrometry. Analyst 139:5835–5842
19. Hu TY, Na WD, Yan X, Su XG (2017) Sensitive fluorescence detection of ATP based on host-guest recognition between near-infrared β-Cyclodextrin-CuInS$_2$ QDs and aptamer. Talanta 165:194–200
20. Song QW, Wang RH, Sun FF, Chen HK, Wang ZK, Na N, Ouyang J (2017) A nuclease-assisted label-free aptasensor for fluorescence turn-on detection of ATP based on the in situ formation of copper nanoparticles. Biosens Bioelectron 87:760–763
21. Xu YX, Li PP, Zhu Y, Tang Y, Chen HY, Zhu XH, Wu CY, Zhang YY, Liu ML, Yao SZ (2022) A fluorescence nanoplatform for the determination of hydrogen peroxide and adenosine triphosphate via tuning of the peroxidase-like activity of CuO nanoparticle decorated UiO-66. Microchim Acta 189:119
22. Tedsana W, Tuntulani T, Ngeontae W (2013) A highly selective turn-on ATP fluorescence sensor based on unmodified cysteamine capped CdS quantum dots. Anal Chim Acta 783:65–73
23. Liu XJ, Lin BX, Yu Y, Cao YJ, Guo ML (2018) A multifunctional probe based on the use of labeled aptamer and magnetic nanoparticles for fluorometric determination of adenosine 5'-triphosphate. Microchim Acta 185:243
24. Zhang LB, Wang EK (2014) Metal nanoclusters: new fluorescent probes for sensors and bioimaging. Nano Today 9:132–157
25. Li JJ, Zhu JJ, Xu K (2014) Fluorescent metal nanoclusters: from synthesis to applications. Trends Anal Chem 58:90–98
26. Yu HZ, Rao B, Jiang W, Yang S, Zhu MZ (2019) The photoluminescent metal nanoclusters with atomic precision. Coord Chem Rev 378:595–617

27. Li D, Chen H, Gao XH, Mei XF, Yang LQ (2021) Development of general methods for detection of virus by engineering fluorescent silver nanoclusters. ACS Sens 6:613–627

28. Xue QS, Li X, Peng YX, Liu P, Peng HB, Niu XH (2020) Polyethylenimine-stabilized silver nanoclusters act as an oxidoreductase mimic for colorimetric determination of chromium (VI). Microchim Acta 187:263

29. Li M, Cai YN, Peng CF, Wei XL, Wang ZP (2021) DNA dendrimer-templated copper nanoparticles: self-assembly, aggregation-induced emission enhancement and sensing of lead ions. Microchim Acta 188:346

30. Zhang M, Guo SM, Li YR, Zuo P, Ye BC (2012) A label-free fluorescent molecular beacon based on DNA-templated silver nanoclusters for detection of adenosine and adenosine deaminase. Chem Commun 48:5488–5490

31. Zhu Y, Hu XC, Shi S, Gao RR, Huang HL, Zhu YY, Lv XY, Yao TM (2016) Ultrasensitive and universal fluorescent aptasensor for the detection of biomolecules (ATP, adenosine and thrombin) based on DNA/Ag nanoclusters fluorescence light-up system. Biosens Bioelectron 79:205–212

32. Xu JN, Wei CY (2017) The aptamer DNA-templated fluorescence silver nanoclusters: ATP detection and preliminary mechanism investigation. Biosens Bioelectron 87:422–427

33. Shen CC, Xia XD, Hu SQ, Yang MH, Wang JX (2014) Silver nanoclusters-based fluorescence assay of protein kinase activity and inhibition. Anal Chem 87:693–698

34. Ge L, Sun XM, Hong Q, Li F (2017) Ratiometric nanocluster beacon: a label-free and sensitive fluorescent DNA detection platform. ACS Appl Mater Interfaces 9:13102–13110

35. Petty JT, Zheng J, Hud NV, Dickson RM (2014) DNA-templated Ag nanocluster formation. J Am Chem Soc 126:5207–5212

36. Diez I, Ras RHA (2011) Fluorescent silver nanoclusters Nanoscale 3:1963–1970

37. Dong FY, Feng ED, Zheng TT, Tian Y (2018) In situ synthesized silver nanoclusters for tracking the role of telomerase activity in the differentiation of mesenchymal stem cells to neural stem cells. ACS Appl Mater Interfaces 10:2051–2057

38. Ouyang XY, Wang MF, Guo LJ, Cui CJ, Liu T, Ren YG, Zhao Y, Ge ZL, Guo XN, Xie G, Li J, Fan CH, Wang LH (2020) DNA nanoribbon-templated self-assembly of ultrasmall fluorescent copper nanoclusters with enhanced luminescence. Angew Chem Int Ed 59:11836–11844

39. Tan HL, Liu BX, Chen Y (2012) Lanthanide coordination polymer nanoparticles for sensing of mercury (II) by photoinduced electron transfer. ACS Nano 6:10505–10511

40. Nhien PQ, Wu PH, Wu CH, Wu JI, Hue BTB, Du BW, Ko FH, Weng CC, Li YK, Lin HC (2021) Multi-stimuli responsive fluorescence of amphiphilic AIEgen copolymers for ultrafast, highly sensitive and selective copper ion detection in water. Sens Actuators B Chem 344:130241

41. Lin YS, Yang ZY, Anand A, Huang CC, Chang HT (2022) Carbon dots with polarity-tunable characteristics for the selective detection of sodium copper chlorophyllin and copper ions. Anal Chim Acta 1191:339311

42. Li YN, Li Y, Wang XY, Su XG (2014) A label-free conjugated polymer-based fluorescence assay for the determination of adenosine triphosphate and alkaline phosphatase. New J Chem 38:4574–4579